

Rare radiative decays of the B_c meson

Wan-Li Ju*, Tianhong Wang, Yue Jiang, Han Yuan, Guo-Li Wang†
Department of Physics, Harbin Institute of Technology, Harbin, 150001, China

Abstract

In this paper, we study the rare radiative processes $B_c \rightarrow D_{sJ}^{(*)}\gamma$ within the Standard Model, where $D_{sJ}^{(*)}$ stands for the meson D_s^* , $D_{s1}(2460, 2536)$ or $D_{s2}^*(2573)$. During the investigations, we consider the contributions from the penguin, annihilation, color-suppressed and color-favored cascade diagrams. Our results show that: 1) the penguin and annihilation contributions are dominant in the branching fractions; 2) for the processes $B_c \rightarrow D_s^*\gamma$ and $B_c \rightarrow D_{s1}(2460, 2536)\gamma$, the effects from the color-suppressed and color-favored cascade diagrams are un-negligible.

arXiv:1511.03805v2 [hep-ph] 25 Jan 2016

*wl_ju_hit@163.com
†gl_wang@hit.edu.cn

1 Introduction

The processes $B_c \rightarrow D_{sJ}^{(*)} \gamma$ in the Standard Model (SM) are emphasized in the recent decades, due to their sensitivity to the new physics (NP). In the existing studies [1–5], the annihilation (Ann) and penguin (Peng) diagrams, as shown in Fig. 1, are paid attention to.

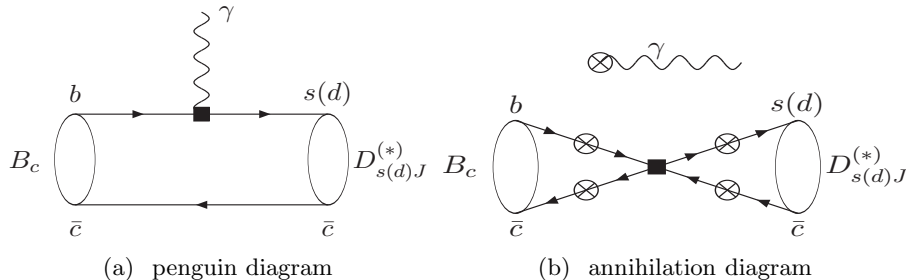


Figure 1: Diagrams of $B_c \rightarrow D_{s(d)J}^{(*)} \gamma$. In annihilation diagram (b) the photon can be emitted from quarks and anti-quarks, denoted by \otimes .

Besides the Ann and Peng effects, the transitions $B_c \rightarrow D_{sJ}^{(*)} \gamma$ are also influenced by long distance (LD) cascade contributions, whose typical diagrams are illustrated in Fig. 2. In order to

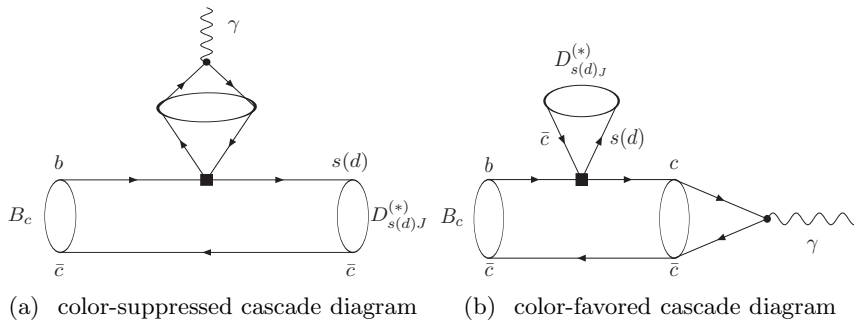


Figure 2: Resonance Cascade Diagrams of $B_c \rightarrow D_{s(d)J}^{(*)} \gamma$.

illustrate their importance to the $B_c \rightarrow D_{sJ}^{(*)} \gamma$ decays, we compare with the $B \rightarrow K^* \gamma$ process. As to the $B \rightarrow K^* \gamma$ transition, its SD contribution is dominated by the penguin diagrams, while the color-suppressed (CS) diagrams are the dominant LD influences¹. According to the estimation in Ref. [6], the CS diagrams influence the Peng ones by 12% in the branching ratio of the $B \rightarrow K^* \gamma$ transition. Thus, the CS diagrams are un-negligible in the $B \rightarrow K^* \gamma$ case. Considering that the typical Peng and CS diagrams for $B \rightarrow K^* \gamma$ process are topologically similar to the $B_c \rightarrow D_{sJ}^{(*)} \gamma$ ones, the CS effects may also influence the Peng amplitudes un-negligibly in $B_c \rightarrow D_{sJ}^{(*)} \gamma$ cases. So it is interesting to consider the CS contributions in the $B_c \rightarrow D_{sJ}^{(*)} \gamma$ channels.

¹Their typical diagrams are identical to Fig. 1 (a) and Fig. 2 (a) respectively if the spectator \bar{c} quarks are replaced by the \bar{u} or \bar{d} quark.

In addition to the CS diagrams, the color-favored (CF) ones also participant in the $B_c \rightarrow D_{sJ}^{(*)}\gamma$ processes. In an approximate sense, the CF amplitudes are 3 times larger than the CS ones due to their color factors. This makes the CF amplitudes more crucial. Therefore, when the $B_c \rightarrow D_{sJ}^{(*)}\gamma$ transitions are studied, it is also interesting to include the CF influences.

Consequently, we are motivated to investigate the $B_c \rightarrow D_{sJ}^{(*)}\gamma$ decays including the Peng, Ann, CS and CF diagrams.

During the investigations, the hadronic matrix elements are involved. In Refs. [1, 2], the hadronic matrix element corresponding to the penguin diagram is estimated by means of the perturbative QCD (pQCD), while the annihilation one is analyzed using the effective formalism [7]. In Ref. [3], the penguin hadronic current is obtained in the relativistic independent quark model (RIQM), while the annihilation one is evaluated by investigating the $B_c \rightarrow M^*\gamma \rightarrow D_s^*\gamma$ processes, where M^* stands for the virtual intermediate state. In Refs. [4, 5], both the penguin and annihilation hadronic currents are computed in QCD sum rules (QCDSR). However, in this paper, we use the hadronic currents in Refs. [8, 9], which are obtained by the Bethe-Salpeter (BS) method [10–15]. The BS method has several particular features. First, in this method, the wave functions are obtained by solving the BS equations and have complete relativistic structure. Second, the Mandelstam Formalism [16] is employed for calculating the hadronic matrix elements, which keeps the relativistic effects from both the kinematics and the dynamics. Third, the BS Ann hadronic currents are effective for all physical region, without any un-physical singularities. Fourth, as proved in Ref. [9], the BS annihilation currents satisfy the gauge-invariance condition, no matter what J^P s of the initial and final mesons are. More important, in our previous works [17–19], the B decays and other B_c transitions are calculated within the BS method. Most of them are in good agreement with the experimental data. Therefore, in this paper, we choose the BS hadronic currents to calculate $B_c \rightarrow D_{sJ}^{(*)}\gamma$ processes.

This paper is organized as follows. In Section 2, we elucidate the theoretical details of the effective hamiltonian and the hadronic transition matrix elements. And Section 3 is devoted to presenting the numerical results and discussions. In Section 4, we draw our conclusion.

2 Theoretical Details

In this part, we introduce the theoretical details on the calculations of $B_c \rightarrow D_{sJ}^{(*)}\gamma$ decays, which includes their transition amplitudes and the involved hadronic currents.

2.1 Transition Amplitudes

From the low energy effective theory [20], the transition amplitude for the $b \rightarrow s(d)\gamma$ process (corresponding to Fig. 1 (a)) is

$$\mathcal{M}_{P_{eng}} = i \frac{eG_F}{4\sqrt{2}\pi^2} m_b V_{ts(d)}^* V_{tb} C_{7\gamma}^{\text{eff}} W_{P_{eng}}^\mu \epsilon_{\gamma\mu}^*, \quad (1)$$

where e stands for the electron charge magnitude and G_F denotes Fermi coupling constant. m_b is the mass of b quark, while $V_{q_1 q_2}$ represents the CKM matrix element. ϵ_γ stands for the polarization vector of photon.

$C_{7\gamma}^{\text{eff}}$ is the effective Wilson coefficient, which can be obtained from the summation of the Wilson coefficients multiplying the same hadronic matrix element. In this paper, we take $C_{7\gamma}^{\text{eff}} = -0.313$ [21]. In Eq. (1), we also define the penguin hadronic matrix element as

$$W_{P_{eng}}^\mu \equiv \langle f | \bar{s}(\bar{d}) i\sigma^{\mu\nu} (1 + \gamma_5) b | i \rangle Q_\nu,$$

where $\sigma^{\mu\nu} \equiv i[\gamma^\mu, \gamma^\nu]/2$ and $Q \equiv P_i - P_f$. $P_i(P_f)$ stands for the momentum of the initial (final) meson.

For the Ann transition amplitude, from the factorization hypothesis [22], we have

$$\mathcal{M}_{Ann} = V_{cb} V_{cs(d)}^* \frac{ieG_F}{\sqrt{2}} a_1^{\text{eff}} W_{Ann}^\mu \epsilon_{\gamma\mu}^*, \quad (2)$$

where W_{ann}^μ is the annihilation hadronic current. It can be expressed as

$$W_{Ann}^\mu = \int dx e^{-iq \cdot x} \langle f | T [O_w(0), J_{\text{em}}^\mu(x)] | i \rangle,$$

where $O_w \equiv \{\bar{c}\gamma^\nu(1 - \gamma_5)b\} \{\bar{s}\gamma^\nu(1 - \gamma_5)c\}$ and $J_{\text{em}}^\mu = Q_q \bar{q}\gamma^\mu q$. Here Q_q stands for the charge of the quark q .

In Eq. (2), the effective coefficient a_1^{eff} is introduced. In this paper, we follow the estimations of QCDSR [23] and take the following set of parameters (Here we also give the numerical value of a_2^{eff} , which will be used in the \mathcal{M}_{CS} calculations.)

$$a_1^{\text{eff}} = 1.14, \quad a_2^{\text{eff}} = -0.20. \quad (3)$$

In recent years, this set of parameters is widely used in the calculations of the B_c non-leptonic decays [24–29].

As to the CS transition amplitude for $B_c \rightarrow D_{sJ}^{(*)}\gamma$ processes, similarly to the $B \rightarrow K^*\gamma$ case, it reads [6]

$$\mathcal{M}_{CS} = i \frac{G_F}{\sqrt{2}} \frac{2e}{3} V_{cb} V_{cs(d)}^* a_2^{\text{eff}} \sum_{V=J/\psi, \psi(2S)\dots} \{ \kappa^2 f_V^2 W_{CS}^\mu \epsilon_{\gamma\mu}^* \}, \quad (4)$$

where the CS hadronic matrix element W_{CS}^μ is defined as $W_{CS}^\mu \equiv \langle f|\bar{s}(\bar{d})\gamma^\mu(1-\gamma_5)b|i\rangle$. In Eq. (4), V denotes the intermediate vector meson and f_V is the according decay constant. Conventionally, we have $\langle 0|\bar{c}\gamma^\mu c|V\rangle = M_V f_V \epsilon_V^\mu$. In this paper, we only consider the contributions for $V = J/\psi$ and $\psi(2S)$. The effects from higher charmonia are suppressed by their small decay constants, while the contributions from ρ , ω and ϕ are suppressed by either their CKM matrix elements $V_{ub}V_{us}^* \sim A\lambda^4$ [32] or the small Wilson coefficients $C_3 - C_6$ [20]. In Eq. (4), the suppression factor κ is also introduced in order to describe the off-shell behaviors of J/ψ and $\psi(2S)$ mesons. In this paper, we follow the discussions in Refs. [6, 30] and take $\kappa = 0.63$.

Based on the derivations in Refs. [8, 31], the CF amplitude is

$$\mathcal{M}_{CF} = i\frac{G_F}{\sqrt{2}}\frac{2e}{3}V_{cb}V_{cs(d)}^*a_1^{\text{eff}} \sum_{V=J/\psi,\psi(2S)} \{\epsilon_{\gamma\mu}^* \frac{\kappa^2 f_f f_V M_f}{M_V} W_{CF}^\mu\}, \quad (5)$$

where M_V and M_f are the masses of the intermediate vector and final mesons, respectively. f_f is the decay constant of the final meson. Here we also only consider the $V = J/\psi, \psi(2S)$ contributions. The $V = \rho, \omega, \phi$ case is not relevant to the CF amplitudes, while the influences for the higher charmonia are suppressed by their smaller decay constants.

In Eq. (5), f_f and W_{CF} are also introduced. Conventionally, we have $\langle f|\bar{s}(\bar{d})\gamma_\mu(1-\gamma_5)c|0\rangle = M_f f_f \epsilon_{f\mu}^*$, and the CF hadronic current is defined as $W_{CF}^\mu \equiv \langle V|\bar{c}\gamma^\nu(1-\gamma_5)b|i\rangle \epsilon_{f\nu}^* \epsilon_V^\mu$. Hereafter $\epsilon_{f(V)}$ denotes the polarization vector of the final (intermediate vector) meson.

Finally, based on the expressions in Eqs. (1,2,4,5), the total transition amplitude reads

$$\mathcal{M}_{Total} = \mathcal{M}_{Peng} + \mathcal{M}_{Ann} + \mathcal{M}_{CS} + \mathcal{M}_{CF}.$$

2.2 Form Factors

In the previous subsection, we have defined the hadronic matrix elements W_{Peng} , W_{Ann} , W_{CS} and W_{CF} . Considering the Lorentz invariance, these hadronic currents can be expressed in

terms of form factors,

$$\begin{aligned}
W^\mu_{Peng}(P \rightarrow V_\perp, A_\perp) &= -iT_1^{V,A} \epsilon^{\mu\epsilon_f^* Q P_+} + T_2^{V,A} P_+ \cdot Q \epsilon_f^{\mu*}, \\
W^\mu_{Ann}(P \rightarrow V_\perp, A_\perp) &= (M_i - M_f) \left\{ T_{1ann}^{V,A} M_i^2 \epsilon_f^{\mu*} + \frac{1}{2} i V_{ann}^{V,A} \epsilon^{\mu\epsilon_f^* Q P_+} \right\}, \\
W^\mu_{CS}(P \rightarrow V_\perp, A_\perp) &= \frac{iV^{V,A}}{M_i + M_f} \epsilon^{\mu\epsilon_f^* Q P_+} - (M_i + M_f) A_1^{V,A} \epsilon_f^{\mu*}, \\
W^\mu_{CF}(P \rightarrow V_\perp, A_\perp) &= (M_i - M_f) \left\{ T_{1CF}^{V,A} M_i^2 \epsilon_f^{\mu*} + \frac{1}{2} i V_{CF}^{V,A} \epsilon^{\mu\epsilon_f^* Q P_+} \right\}, \\
W^\mu_{Peng}(P \rightarrow T_\perp) &= -i \frac{T_1^T}{M_f} (\epsilon_{\alpha\beta}^T)^* Q^\beta \epsilon^{\mu\alpha Q P_+} + \frac{T_2^T}{M_f} P_+ \cdot Q (\epsilon_T^{\mu\beta})^* Q_\beta, \\
W^\mu_{Ann}(P \rightarrow T_\perp) &= (M_i - M_f) \left\{ T_{1ann}^T \frac{M_i^2}{M_f} (\epsilon_T^{\mu\alpha})^* Q_\alpha + \frac{1}{2} i \frac{V_{ann}^T}{M_f} (\epsilon_{\alpha\beta}^T)^* Q^\beta \epsilon^{\mu\alpha Q P_+} \right\}, \\
W^\mu_{CS}(P \rightarrow T_\perp) &= \frac{iV^T}{(M_i + M_f) M_f} (\epsilon_{\alpha\beta}^T)^* Q^\beta \epsilon^{\mu\alpha Q P_+} - \frac{M_i + M_f}{M_f} A_1^T (\epsilon_T^{\mu\alpha})^* Q_\alpha,
\end{aligned} \tag{6}$$

where V_\perp, A_\perp and T_\perp denote the transversely polarized final vector, axial-vector and tensor mesons, respectively. M_i is the mass of the initial meson, while P_+ is defined as $P_+ \equiv P_i + P_f$. $V_{(ann,CF)}^{V,A,T}$, $A_1^{V,A,T}$, $T_{1(ann,CF)}^{V,A,T}$ and $T_2^{V,A,T}$ are form factors. In our previous works [8, 9], these form factors have been calculated in the BS method. In this paper, we use the results directly.

3 Numerical Results and Discussions

In order to calculate the processes $B_c \rightarrow D_{sJ}^{(*)} \gamma$, we need to specify the inputs. In this paper, the masses and the lifetimes of B_c , J/ψ , $\psi(2S)$ and $D_{sJ}^{(*)}$ are taken from Particle Data Group (PDG) [32], as well as the values of α_{em} , G_F and V_{CKM} . The decay constants $f_{J/\psi}$ and $f_{\psi(2S)}$ can be extracted from the branching widths $\Gamma(J/\psi \rightarrow e^+ e^-) = 5.55$ keV and $\Gamma(\psi(2S) \rightarrow e^+ e^-) = 2.35$ keV [32], respectively. And the decay constants $f_{D_{sJ}^{(*)}}$ can be found in our previous works [13, 14]. Using these inputs and Eqs. (1-2,4-5) we can obtain the branching fractions of the $B_c \rightarrow D_{sJ}^{(*)} \gamma$ decays. In the following paragraphs, we will present the numerical results and discuss them.

The results of the $B_c \rightarrow D_s^* \gamma$ decay are listed in Table. 1. $Br_{Peng(Ann,CS,CF)}$ stands for the branching fraction where only $\mathcal{M}_{Peng(Ann,CS,CF)}$ contributes. $Br_{Peng+Ann(CS)}$ is obtained from $\mathcal{M}_{Peng} + \mathcal{M}_{Ann(CS)}$, while Br_{LD} represents the branching ratio including only the \mathcal{M}_{CS} and \mathcal{M}_{CF} influences. $Br_{Peng+Ann+CF}$ includes the \mathcal{M}_{Peng} , \mathcal{M}_{Ann} and \mathcal{M}_{CF} influences. Br_{Total} contains the \mathcal{M}_{Peng} , \mathcal{M}_{Ann} , \mathcal{M}_{CS} and \mathcal{M}_{CF} contributions.

First, as shown in Table. 1, our results satisfy the relationship $Br_{Peng} + Br_{Ann} < Br_{Peng+Ann}$. This relationship indicates the constructive interference between \mathcal{M}_{Peng} and \mathcal{M}_{Ann} . The similar situation can also be found in the results of Refs. [2–4]. Second, one may note that Br_{CS} is much

Table 1: Branching fractions of the decay $B_c \rightarrow D_s^* \gamma$.

	This paper	pQCD [1]	pQCD [2]	RIQM[3]	QCDSR[4]
Br_{Peng}	1.5×10^{-6}	2.2×10^{-7}	3.3×10^{-6}	2.4×10^{-5}	3.5×10^{-6}
Br_{Ann}	4.3×10^{-6}	7.4×10^{-7}	4.4×10^{-6}	4.5×10^{-5}	1.6×10^{-5}
Br_{CS}	1.1×10^{-8}				
Br_{CF}	6.8×10^{-7}				
$Br_{\text{Peng+Ann}}$	9.6×10^{-6}	7.0×10^{-7}	1.0×10^{-5}	1.4×10^{-4}	2.5×10^{-5}
$Br_{\text{Peng+CS}}$	1.7×10^{-6}				
Br_{LD}	5.2×10^{-7}				
$Br_{\text{Peng+Ann+CF}}$	5.8×10^{-6}				
Br_{Total}	6.3×10^{-6}				

smaller than Br_{CF} . This can be understood from the following facts: 1) the CS hadronic matrix element is smaller than the CF one; 2) according to Eqs. (4-5), the CS amplitude is proportional to a_2^{eff} , while the CF one refers to a_1^{eff} . From Eq. (3), we have the relationship $a_2^{\text{eff}} \ll a_1^{\text{eff}}$. Hence, from Table. 1 we see the tiny Br_{CS} . Third, if we compare Br_{Peng} with $Br_{\text{Peng+CS}}$, it is observed that the CS amplitude can influence the Peng one by $\sim 10\%$ in the branching fraction. This is similar to the $B \rightarrow K^* \gamma$ case and in agreement with our estimation in Introduction. Fourth, when CS and CF effects are both included, our Br_{Total} is nearly two thirds of $Br_{\text{Peng+Ann}}$. This implies that in the $B_c \rightarrow D_s^* \gamma$ process, the LD contributions are un-negligible.

Besides, as listed in Table. 1, there are other theoretical predictions on the branching fractions Br_{Peng} and Br_{Ann} . One may note that there is a large discrepancy between the results of various theoretical approaches. Here we try to analyze the reasons.

- Case of Br_{Peng} . As seen from Table. 1, there are five groups calculating Br_{Peng} .
 - In Refs. [1, 2], the same framework, ‘‘PQCD’’ [33], is employed. The reason for their different numerical results is that they use different $C_{7\gamma}^{\text{eff}}$. For instance, in Ref. [2], the Wilson coefficient $C_{7\gamma}^{\text{eff}}$ is obtained neglecting the mixing of $O_{7\gamma}$ with other operators, while in Ref. [1], this approximation is not employed.
 - In Ref. [3], Br_{Peng} s are calculated through RIQM. This method has two particular features, which makes Br_{Peng} in Ref. [3] different from the ones in Refs. [1, 2]. First, the Peng transition amplitude can be expressed as $\Phi_f \otimes O_{7\gamma} \otimes \Phi_i$, while in Refs. [1, 2] the single gluon should be exchanged within the hard kernel. Second, in Ref. [3], the Gaussian wave functions are employed, while in Refs. [1, 2], the non-relativistic limit is used, namely, $\Phi_i(x) \sim \delta(x - m_c/M_{B_c})$ and $\Phi_f(x) \sim \delta(x - (M_f - m_c)/M_f)$.
 - In this paper, Br_{Peng} s are obtained from the BS method. By this method, the Peng

amplitude are calculated in the Mandelstam form, while the initial and final wave functions $\Phi_{i,f}$ are dealt including the relativistic influences. To be specific, in BS method, the traditional Gaussian wave functions are abandoned. Instead, they are solved by the BS equations [12–15]. Besides, for the mesons with definite parity and charge, our wave functions have the complete relativistic structures. The components caused by the relative momenta are not neglected.

- In Ref. [4], Br_{Peng} is evaluated by the QCDSR. This method is a quite different framework from the ones in this paper and Refs. [1–3]. In QCDSR, the Peng amplitude is related to the correlation functions and these correlation functions are calculated with the help of the operator product expansion (OPE). Unlike the PQCD, RIQM and BS methods, where the LD fluctuations are contained in the wave functions, the LD interactions in QCDSR are described by the photon distribution amplitudes and the quark (gluon) condensate inputs. It is believed that our result in Br_{Peng} should be very close to the one in Ref. [4] if the following conditions are satisfied: 1) the exact photon distribution amplitudes are employed; 2) the higher order effects in OPE are small enough; 3) our BS wave functions are obtained rigorously; 4) all contributions beyond our factorization formula are negligible. But at this moment, they are practically involved. For instance, our wave functions are solved under the instantaneous approximations [34], while only leading power contributions are discussed in Ref. [4]. So if more accurate hadronic matrix elements are wanted, more works are still needed in the future.
- Case of Br_{Ann} . Here we attempt to analyze the reasons for the different Br_{Ann} s.
 - In Refs. [1, 2], Br_{Ann} s are both computed within the effective formalism [7]. The difference between them is caused by their different inputs, namely, a_1^{eff} .
 - As shown in Table. 1, the result in Ref. [2] is in agreement with ours. This is because 1) the parameter a_1^{eff} used in Ref. [2] is close to ours; 2) if the expansion in $\Lambda_{\text{QCD}}/M_{B_c}$ is performed in our calculations and only the leading power contributions are kept, our framework is equivalent to the effective formalism [7].
 - Table. 1 also shows that Br_{Ann} in Ref. [3] is almost one order smaller than ours. In Ref. [3], the Ann amplitudes are obtained by calculating $B_c \rightarrow B_c^* \gamma \rightarrow D_s^* \gamma$ and $B_c \rightarrow D_s \rightarrow D_s^* \gamma$ transitions. However, in this paper, we deal with this problem in the parton level.

- In Table. 1, we also list the results in QCDSR [4]. The differences and relations between QCDSR and the BS method are mentioned before. Here we do not discuss them.

In the paragraphs above, we have discussed the discrepancies between the results of different approaches. It is hard to say which method is the most accurate one at this time, because each is based on the particular hypothesis or expansion and has advantages in different aspects. Therefore, in the future, more works on the hadronic currents are still needed.

Table 2: Branching fractions of the decay $B_c \rightarrow D_{s1}(2460)\gamma$.

	This paper	QCDSR[5]
Br_{Peng}	1.8×10^{-6}	1.8×10^{-8}
Br_{Ann}	1.1×10^{-6}	2.2×10^{-5}
Br_{CS}	1.6×10^{-8}	
Br_{CF}	5.8×10^{-7}	
$Br_{\text{Peng+Ann}}$	5.6×10^{-6}	2.4×10^{-5}
$Br_{\text{Peng+CS}}$	2.1×10^{-6}	
Br_{LD}	4.1×10^{-7}	
$Br_{\text{Peng+Ann+CF}}$	2.8×10^{-6}	
Br_{Total}	3.2×10^{-6}	

In Table. 2, we show the branching fractions of the decay $B_c \rightarrow D_{s1}(2460)\gamma$. One may note that the $B_c \rightarrow D_{s1}(2460)\gamma$ transition is in a rather similar situation to the $B_c \rightarrow D_s^*\gamma$ case. Hence, we only emphasize the following two points. First, if only Ann and Peng contributions are considered, our result $Br_{\text{Peng+Ann}}$ is almost a fifth of the one in Ref. [5]. Second, when the LD influences are added, the total branching fraction $Br_{\text{Total}}(B_c \rightarrow D_{s1}(2460)\gamma)$ reduces un-negligibly.

Table 3: Branching fractions of the $B_c \rightarrow D_{s1}(2536)\gamma$ and $B_c \rightarrow D_{s2}^*\gamma$ decays.

	$B_c \rightarrow D_{s1}(2536)\gamma$	$B_c \rightarrow D_{s2}^*\gamma$
Br_{Peng}	1.8×10^{-7}	1.3×10^{-6}
Br_{Ann}	5.3×10^{-7}	5.6×10^{-7}
Br_{CS}	6.1×10^{-10}	3.1×10^{-9}
Br_{CF}	3.8×10^{-8}	-
$Br_{\text{Peng+Ann}}$	1.1×10^{-6}	2.4×10^{-6}
$Br_{\text{Peng+CS}}$	2.1×10^{-7}	1.2×10^{-6}
Br_{LD}	3.0×10^{-8}	3.1×10^{-9}
$Br_{\text{Peng+Ann+CF}}$	8.2×10^{-7}	2.4×10^{-6}
Br_{Total}	8.6×10^{-7}	2.2×10^{-6}

In Table. 3, we show the results of the $B_c \rightarrow D_{s1}(2536)\gamma$ and $B_c \rightarrow D_{s2}^*\gamma$ decays. As to the $B_c \rightarrow D_{s1}(2536)\gamma$ process, except their smaller branching ratios, we see the similar behaviors to the $B_c \rightarrow D_s^*\gamma$ decay. But for the $B_c \rightarrow D_{s2}^*\gamma$ case, their situations is quite different. First, its Br_{Peng} is almost two times bigger than Br_{Ann} . This is because that for the $B_c \rightarrow D_{s2}^*\gamma$ transitions, the Ann hadronic form factors are much smaller than the Peng ones, as shown in Ref. [9]. Second, there is no CF contribution in $B_c \rightarrow D_{s2}^*\gamma$ decay. This can be understood from Eq. (5). In Eq. (5), the factor f_f appears. When the transition $B_c \rightarrow D_{s2}^*\gamma$ is referred, the conservation of angular momentum makes $f_{D_{s2}^*}$ vanish. Hence, $\mathcal{M}_{CF}^\mu(B_c \rightarrow D_{s2}^*\gamma) = 0$. Third, we see this channel is influenced by the LD contributions imperceptibly. This implies that if only the SD contributions are interesting, the $B_c \rightarrow D_{s2}^*\gamma$ decay provides clearer laboratory than $B_c \rightarrow D_s^*\gamma$ and $B_c \rightarrow D_{s1}(2460, 2536)\gamma$ processes.

4 Conclusion

In this paper, considering the penguin, annihilation, color-suppressed and color-favored cascade diagrams, we calculate the processes $B_c \rightarrow D_{sJ}^{(*)}\gamma$ in the Standard Model. Our conclusions include:

1. The processes $B_c \rightarrow D_s^*\gamma$ and $B_c \rightarrow D_{s1}(2460, 2536)\gamma$ receive un-negligible contributions from CS and CF diagrams. When these decays are investigated, including the LD effects is necessary.
2. The transitions $B_c \rightarrow D_{s2}^*\gamma$ is affected by the LD diagrams slightly. Hence, if only the short distance interactions are interested, this channel offers much clearer laboratories than the $B_c \rightarrow D_s^*\gamma$ and $B_c \rightarrow D_{s1}(2460, 2536)\gamma$ processes.
3. In different methods, the results on $Br_{\text{Peng+Ann}}$ are quite different. From this, more discussions and more precise calculations are still needed in the future.

Acknowledgments

This work was supported in part by the National Natural Science Foundation of China (NSFC) under Grant No. 11405037, No. 11575048 and No. 11505039, and in part by PIRS of HIT No.A201409.

References

- [1] G. -R. Lu, C. Yue, Y. -G. Cao, Z. -H. Xiong and Z. -J. Xiao, Phys. Rev. D **54**, 5647 (1996) [hep-ph/9609271].
- [2] D. -S. Du, X. -L. Li and Y. -D. Yang, Phys. Lett. B **380**, 193 (1996) [hep-ph/9603291].
- [3] N. Barik, S. Naimuddin, S. Kar and P. C. Dash, Phys. Rev. D **63**, 014024 (2001).
- [4] K. Azizi and V. Bashiry, Phys. Rev. D **76**, 114007 (2007) [arXiv:0708.2068 [hep-ph]].
- [5] K. Azizi, N. Ghahramani and A. R. Olamaei, Phys. Rev. D **87**, 016013 (2013) [arXiv:1207.1676 [hep-ph]].
- [6] Y. Y. Keum, M. Matsumori and A. I. Sanda, Phys. Rev. D **72**, 014013 (2005) [hep-ph/0406055].
- [7] H. -Y. Cheng, C. -Y. Cheung, G. -L. Lin, Y. C. Lin, T. -M. Yan and H. -L. Yu, Phys. Rev. D **51**, 1199 (1995) [hep-ph/9407303].
- [8] W. -L. Ju, G. -L. Wang, H. -F. Fu, T. -H. Wang and Y. Jiang, JHEP **1404**, 065 (2014) [arXiv:1307.5492 [hep-ph]].
- [9] W. L. Ju, G. L. Wang, H. F. Fu, Z. H. Wang and Y. Li, JHEP **1509**, 171 (2015) [arXiv:1407.7968 [hep-ph]].
- [10] C. H. Chang, J. K. Chen, X. Q. Li and G. L. Wang, Commun. Theor. Phys. **43**, 113 (2005) doi:10.1088/0253-6102/43/1/023 [hep-ph/0406050].
- [11] C. H. Chang, J. K. Chen and G. L. Wang, Commun. Theor. Phys. **46**, 467 (2006). doi:10.1088/0253-6102/46/3/017
- [12] G. Cvetic, C. S. Kim, G. L. Wang and W. Namgung, Phys. Lett. B **596**, 84 (2004) doi:10.1016/j.physletb.2004.06.092 [hep-ph/0405112].
- [13] G. L. Wang, Phys. Lett. B **633**, 492 (2006) doi:10.1016/j.physletb.2005.12.005 [math-ph/0512009].
- [14] G. L. Wang, Phys. Lett. B **650**, 15 (2007) doi:10.1016/j.physletb.2007.05.001 [arXiv:0705.2621 [hep-ph]].
- [15] G. L. Wang, Phys. Lett. B **674**, 172 (2009) doi:10.1016/j.physletb.2009.03.030 [arXiv:0904.1604 [hep-ph]].

- [16] S. Mandelstam, Proc. Roy. Soc. Lond. A **233**, 248 (1955). doi:10.1098/rspa.1955.0261
- [17] C. H. Chang, H. F. Fu, G. L. Wang and J. M. Zhang, Sci. China Phys. Mech. Astron. **58**, 071001 (2015) [arXiv:1411.3428 [hep-ph]].
- [18] H. F. Fu, G. L. Wang, Z. H. Wang and X. J. Chen, Chin. Phys. Lett. **28**, 121301 (2011) doi:10.1088/0256-307X/28/12/121301 [arXiv:1202.1221 [hep-ph]].
- [19] Y. Jiang, G. L. Wang, T. Wang, W. L. Ju and H. F. Fu, Int. J. Mod. Phys. A **28**, 1350110 (2013). doi:10.1142/S0217751X13501108
- [20] G. Buchalla, A. J. Buras and M. E. Lautenbacher, Rev. Mod. Phys. **68**, 1125 (1996) [hep-ph/9512380].
- [21] A. Faessler, T. Gutsche, M. A. Ivanov, J. G. Korner and V. E. Lyubovitskij, Eur. Phys. J. direct C **4**, 18 (2002) [hep-ph/0205287].
- [22] M. Bauer, B. Stech and M. Wirbel, Z. Phys. C **34**, 103 (1987).
- [23] V. V. Kiselev, A. E. Kovalsky and A. K. Likhoded, Nucl. Phys. B **585**, 353 (2000) [hep-ph/0002127]; V. V. Kiselev, hep-ph/0211021.
- [24] H. -F. Fu, Y. Jiang, C. S. Kim and G. -L. Wang, JHEP **1106**, 015 (2011) [arXiv:1102.5399 [hep-ph]].
- [25] D. Ebert, R. N. Faustov and V. O. Galkin, Phys. Rev. D **82**, 034019 (2010) [arXiv:1007.1369 [hep-ph]].
- [26] H. M. Choi and C. R. Ji, Phys. Rev. D **80**, 114003 (2009) [arXiv:0909.5028 [hep-ph]].
- [27] C. Albertus, Phys. Rev. D **89**, 065042 (2014) [arXiv:1401.1791 [hep-ph]].
- [28] M. A. Ivanov, J. G. Korner and P. Santorelli, Phys. Rev. D **73**, 054024 (2006) [hep-ph/0602050].
- [29] D. Ebert, R. N. Faustov and V. O. Galkin, Phys. Rev. D **68**, 094020 (2003) [hep-ph/0306306].
- [30] E. Golowich and S. Pakvasa, Phys. Rev. D **51**, 1215 (1995) [hep-ph/9408370].
- [31] C. H. Chang, C. D. Lu, G. L. Wang and H. S. Zong, Phys. Rev. D **60**, 114013 (1999) [hep-ph/9904471].

- [32] K. A. Olive *et al.* [Particle Data Group Collaboration], Chin. Phys. C **38**, 090001 (2014).
- [33] G. P. Lepage and S. J. Brodsky, Phys. Rev. D **22**, 2157 (1980).
doi:10.1103/PhysRevD.22.2157
- [34] C. H. Chang and Y. Q. Chen, Phys. Rev. D **49**, 3399 (1994). doi:10.1103/PhysRevD.49.3399